PHYSICAL REVIEW C **88**, 031303(R) (2013)

First observation of ^{15}Be

J. Snyder,[1,2,*] T. Baumann,[1] G. Christian,[1,2,†] R. A. Haring-Kaye,[3] P. A. DeYoung,[4] Z. Kohley,[1,5] B. Luther,[6] M. Mosby,[1,5] S. Mosby,[1,2,‡] A. Simon,[1] J. K. Smith,[1,2] A. Spyrou,[1,2] S. Stephenson,[7] and M. Thoennessen[1,2]

[1]*National Superconducting Cyclotron Laboratory, Michigan State University, East Lansing, Michigan 48824, USA*
[2]*Department of Physics & Astronomy, Michigan State University, East Lansing, Michigan 48824, USA*
[3]*Department of Physics & Astronomy, Ohio Wesleyan University, Delaware, Ohio 43015, USA*
[4]*Department of Physics, Hope College, Holland, Michigan 49422, USA*
[5]*Department of Chemistry, Michigan State University, East Lansing, Michigan 48824, USA*
[6]*Department of Physics, Concordia College, Moorhead, Minnesota 56562, USA*
[7]*Department of Physics, Gettysburg College, Gettysburg, Pennsylvania 17325, USA*

(Received 22 April 2013; revised manuscript received 30 July 2013; published 6 September 2013)

The neutron-unbound nucleus ^{15}Be was observed for the first time. It was populated using neutron transfer from a deuterated polyethylene target with a 59 MeV/u ^{14}Be beam. Neutrons were measured in coincidence with outgoing ^{14}Be particles and the reconstructed decay energy spectrum exhibits a resonance at 1.8(1) MeV. This corresponds to ^{15}Be being unbound by 0.45 MeV more then ^{16}Be thus significantly hindering the sequential two-neutron decay of ^{16}Be to ^{14}Be through this state.

DOI: 10.1103/PhysRevC.88.031303 PACS number(s): 21.10.Dr, 25.60.−t, 29.30.Hs, 27.20.+n

The increased intensities of rare isotope beams has opened up new opportunities to produce and study nuclides beyond the neutron drip line [1]. One- and two-proton removal reactions as well as light-particle transfer reactions have been used to populate unbound nuclei from neutron unbound hydrogen (up to ^{7}H [2]) to fluorine (^{28}F [3]) isotopes. Of recent interest are nuclei that decay by the emission of two neutrons. For example the ground state of ^{16}Be was observed to decay by the emission of two strongly correlated neutrons [4–6] and in ^{26}O indications of two-neutron radioactivity were reported [7].

The analysis of two-proton radioactivity has shown that diproton emission is favorable only when the decay via the sequential emission of two protons is energetically not allowed [8]. For the emission of two neutrons this situation seems to be the case in the decay of the aforementioned case of ^{16}Be, which was observed to be unbound with respect to the emission of two neutrons by 1.35(10) MeV [4]. The search for an intermediate resonance in ^{15}Be was unsuccessful [9]. Spyrou *et al.* populated ^{15}Be using a two-proton removal reaction from ^{17}C. From the nonobservation of any ^{14}Be fragments it was concluded that any populated states of ^{15}Be must be located above the unbound first excited state of ^{14}Be and thus decay by the emission of three sequential neutrons into ^{12}Be.

Presently little is known about ^{15}Be. It has never been demonstrated explicitly to be unbound, however, from the fact that the heavier isotone ^{16}B is unbound [10,11] it can be deduced that ^{15}Be also is unbound with respect to neutron emission. Furthermore, the predicted level structure of ^{15}Be is still uncertain. While early shell-model calculations predicted a $5/2^+$ ground state with an excited $3/2^+$ state at 70 keV [12] more recent calculations with NUSHELLX [13] in the *s-p-sd-pf* model space and the Warburton-Brown *p*-shell (WBP) Hamiltonian [14] resulted in a $3/2^+$ ground state and $5/2^+$ excited state at 300 keV [9]. The two-proton removal reaction from ^{17}C is expected to strongly populate the $3/2^+$ state and not the $5/2^+$ state [9]. In addition, the $3/2^+$ state is also calculated to have a strong spectroscopic overlap with the first unbound excited 2^+ state in ^{14}Be. Thus, the population of the $3/2^+$ state in ^{15}Be would likely lead to a three-neutron sequential decay to ^{12}Be. This scenario was confirmed from the nonobservation of ^{14}Be in the two-proton removal experiment [9].

However, it cannot be ruled out that the $5/2^+$ state is located at a sufficiently low energy to serve as the intermediate state for the sequential two neutron decay of ^{16}Be. In order to search for this state we performed an experiment using neutron transfer from a deuterated polyethylene target, which should not have the high selectivity of the proton removal reaction and thus should populate both the $3/2^+$ and the $5/2^+$ states in^{15}Be.

The experiment was performed at the National Superconducting Cyclotron Laboratory (NSCL) at Michigan State University. A 120 MeV/u ^{18}O primary beam from the Coupled Cyclotron Facility bombarded a 3196 mg/cm^2 ^{9}Be production target. The A1900 fragment separator in conjunction with a 1050 mg/cm^2 aluminum achromatic wedge degrader was used to separate and select for the ^{14}Be secondary beam. The final energy of the beam was 59 MeV/u with a momentum spread of 2%, an intensity of approximately 1000 pps, and a purity of 96.5%. The beam particles were cleanly identified on an event by event basis, using the flight time between two plastic scintillators placed at the A1900 focal plane and just in front of the reaction target. The ^{14}Be beam impinged upon a 435 mg/cm^2 deuterated polyethylene target, where ^{15}Be was produced in a neutron transfer reaction. The unbound ^{15}Be then immediately decayed into ^{14}Be and a neutron.

The ^{14}Be reaction products were deflected by a large-gap dipole magnet [15] set to a magnetic rigidity of 3.55 Tm. Following the large-gap dipole magnet the position and angle information was calculated for the charged particles by interacting with two 30 cm × 30 cm cathode readout drift chambers separated by 1.88 m. Energy loss and total

*snyder@nscl.msu.edu
†Present address: TRIUMF, 4004 Wesbrook Mall, Vancouver, British Columbia V6T 2A3, Canada.
‡Present address: LANL, Los Alamos, NM 87545, USA.

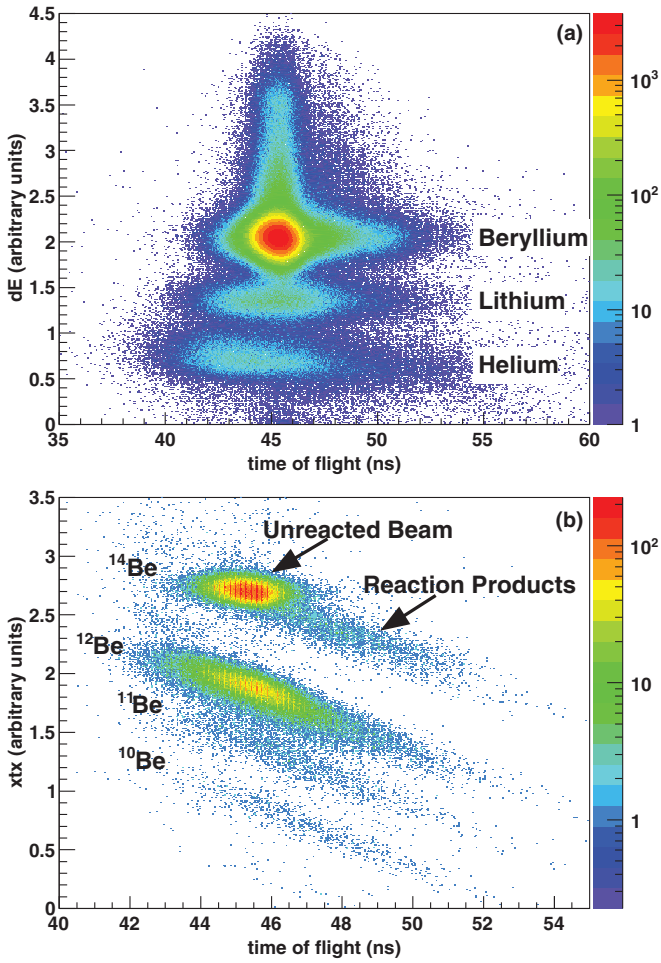

FIG. 1. (Color online) Element, isotope, and ^{14}Be reaction product identification: (a) Energy loss (DE) versus time of flight of the fragments. The different elements are cleanly separated. (b) Isotope identification parameter *xtx* versus time of flight. The identified beryllium isotopes, along with ^{14}Be reaction products are indicated in the figure.

energy were measured in 5 mm and 150 mm thick plastic scintillators, respectively. The energy and momentum vector of the fragments were reconstructed from a transformation matrix based on the magnetic field map using the program COSY INFINITY [16].

Coincident neutrons were measured with the Modular Neutron Array (MoNA) [17,18]. The 144 plastic scintillator detectors of the array were arranged into 18 walls each 80 cm tall. The walls were assembled into two close-packed blocks located at 0° and 23° from the secondary beam direction, with their respective distances from the target being 650 cm and 470 cm. The position of a neutron interaction within the array was determined from the location of the corresponding bar and the time difference between the signals of the photomultiplier tubes attached to each end of the bars. The neutron energy was determined from the time of flight between the reaction target scintillator and the average time of the photomultiplier tube signals of each bar. The momentum vector of each interaction was then reconstructed from the calculated position and energy.

After the dipole magnet, beryllium was identified in an energy loss versus time-of-flight plot as shown in Fig. 1(a), where the energy loss in the 5 mm plastic scintillator is plotted against the flight time from the reaction target to this scintillator. Beryllium, lithium, and helium are cleanly separated. To achieve isotope separation, the technique described in Ref. [19] was used to create an "emittance" parameter *xtx*, which is calculated from the dispersive position and angle after the large-gap dipole magnet. The parameter *xtx* is then plotted versus time of flight to achieve isotopes separation. Figure 1(b) shows the isotopic separation for beryllium. The intense peak in the beryllium band corresponds to the unreacted ^{14}Be beam, the identified isotopes are indicated. The gap corresponds to the absence of unbound ^{13}Be. To minimize the unreacted beam contribution in Fig. 1(b) all events were required to have a coincident neutron detected in MoNA. This allows for the separation of the slower ^{14}Be reaction products from the remaining unreacted beam.

The fact that the unreacted beam could not be separated from the reaction fragments by the sweeper magnet resulted in a large number of random coincidence events in MoNA. Figure 2 shows the neutron time-of-flight spectra where these events appear as a uniform background under the peak of neutrons from the reaction (black points). These events are mostly due to room background γ rays, which trigger the MoNA bars but do not deposit a large amount of energy. An energy threshold of 3 MeV was sufficient to eliminate these γ rays (red points in Fig. 2). In order to select only neutrons from the decay of ^{15}Be, a gate requiring only beam velocity neutrons was applied eliminating the remaining slower neutrons.

The decay energy was calculated from the fragment and neutron energy and momentum vectors. The decay energy spectrum for ^{15}Be shown in Fig. 3 is dominated by a peak near 2 MeV.

A deuterated polyethylene target was selected in order to maximize the number of nuclei and minimize the overall energy loss, which represents the dominant contribution to the overall decay energy resolution. With this target ^{15}Be can be populated by neutron transfer from the deuterons or the carbon nuclei. In order to investigate any possible differences between

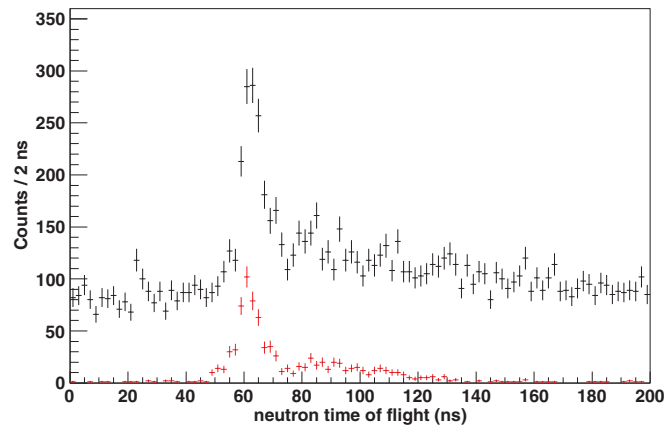

FIG. 2. (Color online) Neutron time of flight. The black data points corresponds to events in coincidence with neutrons and the ^{14}Be reaction products. The red data points also require an energy of at least 3 MeV deposited in the MoNA bars.

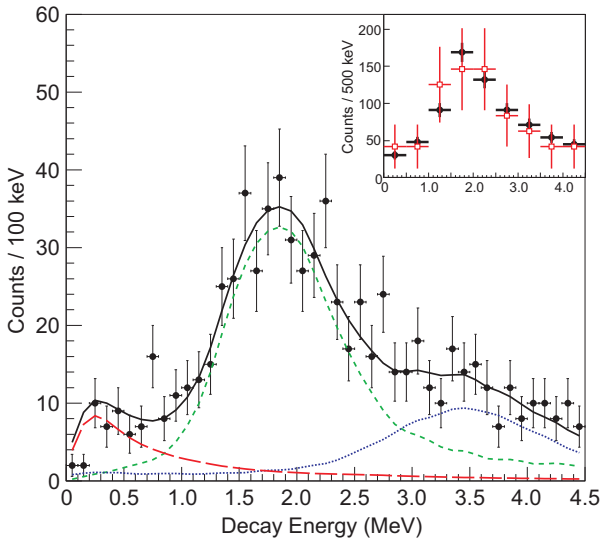

FIG. 3. (Color online) ^{15}Be decay energy spectrum. The data are shown by the circles with statistical error bars. The best fit to the data (solid black line) is a sum of an $l = 2$ resonance (green short-dashed line) and background contributions approximated by $l = 0$ (red long-dashed line) and $l > 0$ (blue dotted line) components. In the inset the decay energy for the deuterated polyethylene target (black solid points) is compared to the carbon target (red open squares). The carbon data is normalized to the same counts as the deuterated polyethylene data.

these two reactions, a 300 mg/cm^2 carbon target was used for 10% (16 hours) of the experiment. As shown in the inset of Fig. 3 the decay energy spectra for the carbon target (red open squares) and the deuterated polyethylene target (black solid points) are statistically identical. This indicates that the invariant mass reconstruction is independent of the reaction mechanism used to populate the state in ^{15}Be.

In order to determine the decay energy of this resonance, Monte Carlo simulations were performed where the incoming beam characteristics, reaction mechanism, and detector resolutions were taken into account. The neutron interactions within MoNA were simulated with GEANT4 [20,21] using the MENATE_R package [22] as described in Ref. [23].

The experimental decay energy spectrum was fitted using an energy-dependent Breit-Wigner distribution assuming an $l = 2$ decay along with a background contribution. The background is most likely due to the population of unbound higher-lying states. Other than the peak close to 2 MeV no other distinct resonance features are apparent, so the background was approximated with a combination $l = 0$ and $l > 0$ component. These contributions were selected to reproduce the background below 1 MeV and above 3 MeV, respectively. The line shapes shown in Fig. 3 were calculated with a scattering length of -2.5 fm and a single resonance at 3.5 MeV with a width of 0.8 MeV. The overall fit was not sensitive to the detailed parametrizations of the background contribution and they should not be interpreted as distinct states in ^{15}Be.

The $l = 2$ resonance energy, width, and normalization, along with the normalization of the two background contributions were free parameters. The best fit to the data was achieved with a resonance energy of 1.8(1) MeV and a width of 575(200) keV along with two background components and is shown by the black solid line in Fig. 3. The individual contributions of the resonance, $l = 0$ and $l > 0$ background contributions are shown by the green short-dashed, red long-dashed, and blue dotted lines, respectively. This observation corresponds to the first identification of the neutron-unbound nucleus ^{15}Be.

Shell-model calculations with NUSHELLX mentioned in the introduction predicted the $3/2^+$ ground state and the $5/2^+$ excited state to be unbound by 2.5 MeV and 2.8 MeV, respectively. It is conceivable that the observed peak corresponds to a sum of both of these states, however this is not required by the data. The extracted width of the single-component fit [575(200) keV] is consistent with the calculated single-particle width of 405 keV.

According to the FRESCO [24] calculations the $5/2^+$ state should be populated more than the $3/2^+$ state by about a factor of 1.5. However, the spectroscopic overlap of the two states with the ground state of ^{14}Be are significantly different. While the $5/2^+$ state has substantial spectroscopic strength (0.44) for decaying to the ground state of ^{14}Be, the ground-state decay branch of the $3/2^+$ state is much weaker (0.07) and it will predominantly decay to the first excited 2^+ state of ^{14}Be with an $l = 0$ transition. Thus, the present peak is tentatively assigned to the $5/2^+$ state. The cross section for populating this state in ^{15}Be by neutron transfer from carbon and deuterium were measured to be 1.1(6) mb and 0.7(5) mb, respectively. These cross sections are consistent with FRESCO calculations. The cross section for the neutron transfer from carbon was calculated to be 0.7 mb using optical potentials derived from ^{12}C induced reaction at 50 MeV/nucleon [25]. For the transfer from deuterium calculations with several different global optical potentials [26–28] resulted in cross sections from 1–2 mb.

The current experiment does not resolve the question of which of the two states corresponds to the ground state. Figure 4 summarizes the experimental status of the neutron-rich beryllium isotopes. The nonobservation of ^{14}Be

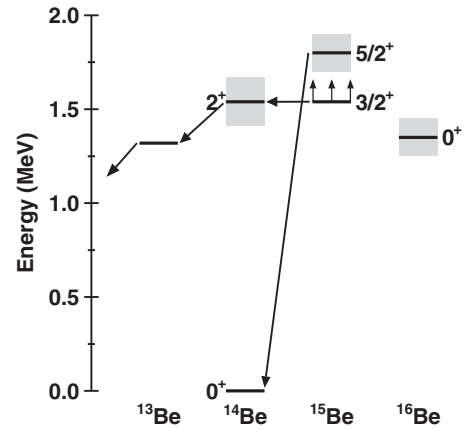

FIG. 4. Partial experimental level scheme for neutron rich beryllium isotopes. The height of the grey boxes represents the uncertainties of the states. The data for the excited state in ^{14}Be is from [29], the lower limit for the $3/2^+$ is from Ref. [9], the ^{15}Be $5/2^+$ state is from the present work and the two-neutron separation energy for ^{16}Be is from Ref. [4].

in the two-proton knockout experiment established a lower limit for the decay energy of the $3/2^+$ state of 1.54 MeV [9]. This state will decay to the unbound first excited 2^+ state of ^{14}Be, which then subsequently will decay via ^{13}Be to the ground state of ^{12}Be. This state will be difficult to observe because it will require the kinematic reconstruction of three neutrons. The present result places the $5/2^+$ state at a decay energy of 1.8(1) MeV. As shown in Fig. 4 this places the ^{15}Be state above the ^{16}Be ground state by 450(140) keV. Using the formalism described in Refs. [30,31] the partial width for the sequential decay of ^{16}Be through this ^{15}Be intermediate state was calculated to be $3.5^{+2.5}_{-1.8}$ keV. This small width is due to the large energy difference of the two states and the angular momentum barrier for this $l = 2$ transition. The previously measured large total width of 800^{+100}_{-200} keV for the decay of ^{16}Be [4] thus cannot be explained with the sequential decay through the $5/2^+$ state in ^{15}Be. In addition to the direct decay, the sequential decay through the still unobserved $3/2^+$ state in ^{15}Be could contribute to the total decay width of ^{16}Be.

In conclusion, we observed the neutron-unbound nucleus ^{15}Be for the first time. It was populated with neutron transfer from a deuterated polyethylene target in inverse kinematics with a radioactive beam of ^{14}Be. ^{15}Be decays by neutron emission to ^{14}Be with a decay energy of 1.8(1) MeV and a spin and parity of $5/2^+$ is tentatively assigned to the state based on shell-model calculations.

The authors gratefully acknowledge the support of the NSCL operations staff for providing a high quality beam. We also wish to thank the Hope Ion Beam Analysis Laboratory for the support with the RBS analysis of the target, and Alexander Volya for help with theoretical calculations. This material is based upon work supported by the Department of Energy National Nuclear Security Administration under Award No. DE-NA0000979 and DOE Award No. DE-FG02-92ER40750. This work was also supported by the National Science Foundation under Grants No. PHY06-06007, No. PHY09-69058, and No. PHY11-02511.

[1] T. Baumann, A. Spyrou, and M. Thoennessen, Rep. Prog. Phys. **75**, 036301 (2012).
[2] A. A. Korsheninnikov *et al.*, Phys. Rev. Lett. **90**, 082501 (2003).
[3] G. Christian *et al.*, Phys. Rev. Lett. **108**, 032501 (2012).
[4] A. Spyrou *et al.*, Phys. Rev. Lett. **108**, 102501 (2012).
[5] F. M. Marqués, N. A. Orr, N. L. Achouri, F. Delaunay, and J. Gibelin, Phys. Rev. Lett. **109**, 239201 (2012).
[6] A. Spyrou *et al.*, Phys. Rev. Lett. **109**, 239202 (2012).
[7] Z. Kohley *et al.*, Phys. Rev. Lett. **110**, 152501 (2013).
[8] B. Blank and M. Ploszajczak, Rep. Prog. Phys. **71**, 046301 (2008).
[9] A. Spyrou *et al.*, Phys. Rev. C **84**, 044309 (2011).
[10] J. D. Bowman, A. M. Poskanzer, R. G. Korteling, and G. W. Butler, Phys. Rev. C **9**, 836 (1974).
[11] R. A. Kryger *et al.*, Phys. Rev. C **53**, 1971 (1996).
[12] N. A. F. M. Poppelier, L. D. Wood, and P. W. M. Glaudemans, Phys. Lett. B **157**, 120 (1985).
[13] B. A. Brown and W. D. M. Rae, NUSHELL (Michigan State University, East Lansing, 2007).
[14] E. K. Warburton and B. A. Brown, Phys. Rev. C **46**, 923 (1992).
[15] M. D. Bird *et al.*, IEEE Trans. Appl. Supercond. **15**, 1252 (2005).
[16] K. Makino and M. Berz, Nucl. Instrum. Methods A **558**, 346 (2005).
[17] B. Luther *et al.*, Nucl. Instrum. Methods A **505**, 33 (2003).
[18] T. Baumann *et al.*, Nucl. Instrum. Methods A **543**, 517 (2005).
[19] G. Christian *et al.*, Phys. Rev. C **85**, 034327 (2012).
[20] S. Agostinelli *et al.*, Nucl. Instrum. Methods A **506**, 250 (2003).
[21] J. Allison *et al.*, IEEE Trans. Nucl. Sci. **53**, 270 (2006).
[22] B. Roeder, "Development and validation of neutron detection simulations for EURISOL," EURISOL Design Study, Report No. 10-25-2008-006-In-beamvalidations.pdf, 2008, pp. 31–44 www.eurisol.org/site02/physics_and_instrumentation/.
[23] Z. Kohley *et al.*, Nucl. Instrum. Methods A **682**, 59 (2012).
[24] I. J. Thompson, Comput. Phys. Rep. **7**, 167 (1988).
[25] J. S. Winfield *et al.*, Phys. Rev. C **39**, 1395 (1989).
[26] J. Bojowald *et al.*, Phys. Rev. C **38**, 1153 (1988).
[27] Y. Han, Y. Shi, and Q. Shen, Phys. Rev. C **74**, 044615 (2006).
[28] H. An and C. Cai, Phys. Rev. C **73**, 054605 (2006).
[29] T. Sugimoto *et al.*, Phys. Lett. B **654**, 160 (2007).
[30] A. Volya and V. Zelevinsky, Phys. Rev. C **74**, 064314 (2006).
[31] A. Volya, EPJ Web of Conferences **38**, 03003 (2012).